Theory and Practice of Science and Technology
2025, VOL. 6, NO. 4, 79-88
DOI: 10.47297/taposatWSP2633-456914.20250604

Analysis of Structural Performance of Underground Complexes at Different Burial Depths

Youbin Bu*, Il-seung Yang, Soon-chul Kim

Dongshin University Naju-si, Jellanam-do, Korea, 58245

ABSTRACT
Since the reform and opening-up policy in China, urban intensification has developed rapidly. The density of large and medium-sized cities has increased sharply, and the degree of population concentration has risen year by year, posing new requirements on the carrying capacity of urban transportation. The trend of urbanization demands a more three-dimensional approach: expanding space underground and upward. Urban road construction has become an important indicator of urban development and a critical "artery" for population flow. Although shallow-buried underground complexes have already been constructed in practice, there is still no mature standardized system. These complexes not only help relieve urban traffic congestion and parking issues but also reduce construction costs. Large-scale underground projects that traditionally required shield tunneling can now be implemented through ground-level construction methods. To study the feasibility of shallow-buried underground complexes, this research analyzes the mechanical performance of the structure to determine reasonable ranges for design parameters. The main focus of this paper is to analyze the mechanical behavior of shallow-buried underground complexes at different burial depths. It compares and analyzes structural performance under static loads at the mid-span, retaining walls, traffic compartment isolation walls, and vulnerable joints to understand how mechanical properties change with burial depth and to determine a reasonable range for soil cover.

KEYWORDS
shallow-buried; complex; underground highway; burial depth

1 Introduction

Urban intensification has progressed rapidly, with increasing density in large and medium-sized cities and growing population concentration. By shifting some urban roads underground, significant relief can be provided to surface traffic. Furthermore, integrating underground traffic with utility corridors not only improves space utilization but also reduces construction costs. The design of a shallow-buried underground complex typically includes a traffic compartment, utility corridor, and mandatory emergency escape passages. Underground projects in China are mainly composed of subway tunnels combined with utility corridors or independent highway tunnels. The combination of highway tunnels with utility corridors remains rare. In this design, the traffic compartment serves as a highway tunnel and must comply with relevant tunnel design standards; the utility corridor follows the specifications for underground utilities, and the escape passage meets functional requirements for emergency evacuation and maintenance. Because the traffic compartment is designed for vehicles, a shallow-buried approach is adopted to seamlessly integrate above-ground and underground traffic. Burial depth affects the structure in two ways: it increases overburden and lateral earth pressure but can reduce the transmission of vehicle vibration loads. Therefore, determining the optimal burial depth is a key research goal.

2 Model Construction

2.1 Section Design

2.1.1 Overall Section Design

Shallow-buried underground complexes are typically constructed using open-cut methods. Based on experiences from cities like Beijing and Shanghai, the overall cross-sectional form is usually rectangular or quasi-rectangular. For example, the open-cut section of the Shanghai Yangtze River Tunnel uses a rectangular section (Figure 2.1), while the underground street crossing on Chang ' an Avenue in Beijing adopts a quasi-rectangular section (Figure 2.2).

To verify model safety, a rectangular cross-section is used in this study.

2.1.2 Traffic Compartment Section Design

According to the design code for urban underground roads [1], if the design speed of an underground road is less than or equal to 60 km/h and it serves small and medium vehicles, the minimum lane width can be 3 m, which satisfies driving requirements and saves underground space. For a design speed of 80 km/h for small vehicles, the lane width can be 3.25 m. Minimum clear heights for urban underground roads vary across cities like Beijing and Shanghai, with limits such as 2.5

m, 3.0 m, 3.2 m, and 3.5 m. Table 2.1 shows the standard values, and Table 2.2 specifies the design speeds for different urban road levels.

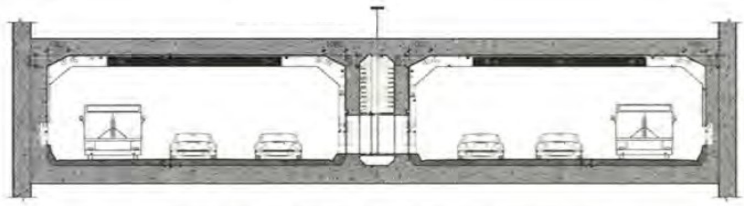

Figure 2.1 Cross section layout of Shanghai Yangtze River Tunnel (open cut section)

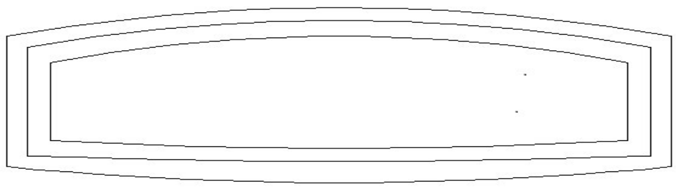

Figure 2.2 Underground crossing street, Chang'an Street, Beijing

Table 2.1 Minimum clear height of urban underground road

Types of Roads	Type of Traveling Traffic	Clear Height(m)
Motor Vehicle Lane	Small Passenger Car	3.5
	All Types of Motor Vehicles	4.5
Non-motor Vehicles	Non-motor Vehicles	2.5
Pedestrian or Maintenance Passage	Pedestrian	2.5

Table 2.2 Design speed of urban underground roads at all levels

Road Classification	Expressway	Arterial Road	Sub-arterial Road	Collector Road
Design Speed(km/h)	60~100	40~60	30~50	20~40

According to highway tunnel design specifications [2], when a maintenance or pedestrian walkway is present, extra width must be included. If no such walkways are present, an additional clearance of no less than 0.25 m is required between lanes. Figure 2.3 shows the tunnel clearance profile, and Table 2.3 provides the structure's layout and standard dimensions.

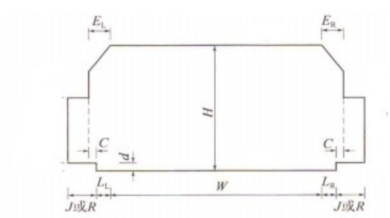

Figure 2.3 Construction clearance of highway tunnel

Table 2.3 Composition and basic width of building gauge and cross section (m)

Highway Classification	Design Speed (km/h)	Lane Width	Left-side Width L_L	Right-side Width L_R	Extra Width C	Maintenance Walkway Width J or Pedestrian Walkway WidthR(Provided on both sides)
First-Class Highway	120	3.75	0.75	1.25	0.50	1.00
	100	3.75	0.75	1.00	0.25	0.75
	80	3.75	0.50	0.75	0.25	0.75
	60	3.50	0.50	0.75	0.25	0.75
Second-Class Highway	80	3.75	0.75	0.75	0.25	1.00
	60	3.50	0.50	0.50	0.25	1.00
Third-Class Highway	40	3.50	0.25	0.25	0.25	0.75
	30	3.25	0.25	0.25	0.25	0.75
Fourth-Class Highway	20	3.00	0.50	0.50	0.25	

2.1.3 Utility Corridor Section Design

According to technical standards for urban utility tunnels, the types, specifications, quantity, and installation requirements of pipes inside the corridor must be considered, and the minimum clear height must not be less than 2.4 m. The main load-bearing sidewalls of the concrete structure should be no less than 250 mm thick, and partition walls for non-load-bearing sides should be no less than 200 mm.

2.2 Structural Model Construction

2.2.1 Structural Section Layout

Based on the overall section rules and standards for the traffic and utility compartments, the structure layout is shown in Figure 2.4.

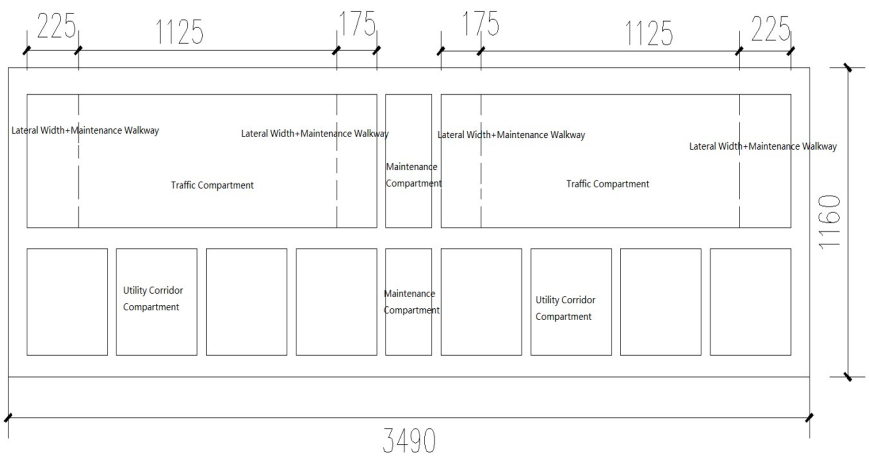

Figure 2.4 Structural section layout(Unit:cm)

The self-weight of concrete is taken as 24 kN/m^3 (density 2400 kg/m^3), using C50 grade concrete. Reinforcement bars are ribbed grade III steel, with diameters of 18 mm, 22 mm, and 25 mm. Soil overburden is uniformly loaded at 18 kN/m^3. Vehicle loads follow the "Highway Engineering Technical Standard." Human load is set at 3.0 kN/m^2, and utility corridor load at 20 kN/m^2. Hydrostatic pressure is calculated using ρgh; lateral soil pressure uses Coulomb's active earth pressure formula. The surrounding rock is grade V cohesive soil with a density of 17 kN/m^3, subgrade reaction coefficient of 150 MPa/m, deformation modulus of 0.004 GPa, Poisson's ratio 0.38, internal friction angle 25°, and cohesion 0.045 MPa.

2.2.2 Concrete Constitutive Model

ABAQUS offers three types of constitutive models for concrete[3]. This study adopts the concrete damage plasticity (CDP) model to simulate the mechanical behavior of the shallow-buried underground complex. The model is based on damage mechanics, assuming concrete failure through either compressive or tensile mechanisms, capturing crushing, cracking, and material degradation. The uniaxial tension and compression behavior is defined using plastic strain curves[4]. Key features of this model include: (1) Compatibility with various loading conditions, unaffected by load type, making it widely applicable. (2) The model remains accurate even when structural cracking occurs, reducing computational errors. (3) Strong convergence characteristics during simulation.

In the CDP model, ABAQUS sets default values of 0 and 1 for tensile and compressive stiffness recovery, respectively. That means, when cracks close under compressive loading, stiffness can recover. However, cracks in shear walls reduce the tensile stiffness, weakening the structure's resistance to further cracking[5].

2.2.3 Reinforcement Constitutive Model

Compared to concrete, the properties of reinforcement steel are more standardized. Four common reinforcement constitutive models are used: ideal elastic-plastic, tri-linear, full-curve, and bi-linear[6]. This study adopts the stress-strain curve shown in Figure 2.5. In the elastic region (steep slope), strain increases minimally before yield stress is reached.

Here, ε_y is the yield strain, f_y is the yield strength, E is the elastic modulus, and E_s is the strain hardening modulus[7], taken as $E_s = 0.01E_0$. Table 2.4 provides plastic parameters for vertical, horizontal, and bolt reinforcement as well as steel plates.

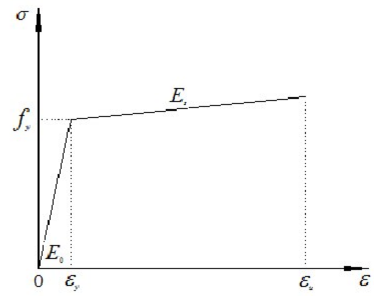

Fig2.5 Constitutive relationship curve of steel

Table2.4 The plastic parameter selection of steel

	Yield Strength/MPa	Ultimate Strength/MPa
Vertical Distribution Reinforcement	400	612
Horizontal Distribution Reinforcement	300	382
Bolt Reinforcement	637	806
Connection Steel Plate	640	800

2.2.4 Solid Elements

The structural model of the shallow-buried underground complex is simulated with solid elements. The concrete walls are modeled using C3D8R elements, shown in Figure 2.6.

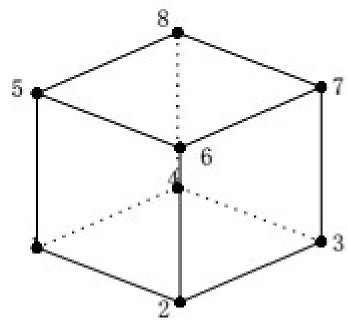

Fig2.6 C3D8R physical unit

2.2.5 Truss Elements

Reinforcement is also critical in this simulation. For precise analysis, truss elements (T3D2) are used to model rebar within the structure[8]. These elements are shown in Figure 2.7.

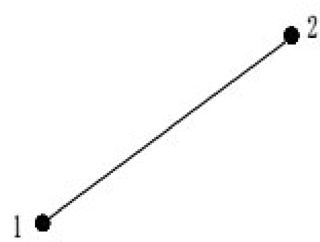

Fig2.7 T3D2 truss unit

3 Experimental Plan and Methods

3.1 Overview

This study analyzes the structural performance of a shallow-buried underground complex at different burial depths. Burial depth is treated as a variable, while other parameters remain constant, using the control variable method. Five burial depths were selected: 0.5m, 0.75m, 1.0m, 1.25m, and 1.5m. For each case, Mises stress, plastic strain, and vertical displacement were analyzed under both loaded and unloaded conditions at the mid-span, span section, and vulnerable nodes.

3.2 Load Parameters

Self-weight Load:

The material density for reinforced concrete is 25–26 kN/m^3. In ABAQUS simulations, vertical self-weight load is applied using gravity acceleration. Crowd Load: Taken as 3.0 kN/m^2 based on the 95th percentile of maximum distributed values during the design life. Utility Tunnel Load: Based on standard layouts and material weights, the utility corridor load is averaged using water density, set as 20 kN/m^2. Hydrostatic Pressure: Calculated using $F=\rho gh$ Surface Overload: Assumed as a uniform load of 10 kN/m^2. Vehicle Load: Based on Di Dongchao's research[9], the equivalent uniformly distributed live load was applied based on soil depth, considering the diffusion of wheel pressure.

1 Burial Depth 0.5m

Vehicle Load:

$$\begin{cases} b_{cx}=b_{tx}+2s\tan\theta=0.6+2\times0.5\times\tan 35^{\circ}=1.3m \\ b_{cy}=b_{ty}+2s\tan\theta=0.2+2\times0.5\times\tan 35^{\circ}=0.9m \end{cases}$$

$$p=\frac{F}{A}=\frac{140}{2\times1.3\times0.9}=59.829\text{kN/m}^2$$

59.829 kN/m2×1.15=68.803kN/m2

Vertical Soil Pressure: 17kN/m^3×0.5m=8.5kN/m^2

Coulomb Earth Pressure:

$$K_a=\frac{\cos^2(\phi-\alpha)}{\cos^2\alpha\cdot\cos(\alpha+\delta)\left[1+\sqrt{\frac{\sin(\phi+\delta)\sin(\phi-\beta)}{\cos(\alpha+\delta)\cos(\alpha-\beta)}}\right]^2}=\frac{\cos^2 25^{\circ}}{\cos^2 25^{\circ}\cdot\cos 37.5^{\circ}\left[1+\sqrt{\frac{\sin 37.5^{\circ}\sin 25^{\circ}}{\cos 37.5^{\circ}\cos 25^{\circ}}}\right]^2}=0.49$$

$$\sigma_a=\gamma HK_a=17\text{kN/}m^3\times12.1m\times0.49=100.793\text{kN/}m^2$$

Surrounding Rock Pressure:

$$e=\gamma\left(H+\frac{1}{2}H_1\right)\tan^2\left(45-\frac{\phi_c}{2}\right)$$
$$=17\text{kN/m}^3\times\left(0.5+\frac{1}{2}\times11.6\right)\text{m}\times\tan^2(45^{\circ}-12.5^{\circ})=43.467\text{kN/m}^2$$

2 Burial Depth 0.75m

Vehicle Load:

$$\begin{cases} b_{cx}=b_{tx}+2s\tan\theta=0.6+2\times0.75\times\tan 35^{\circ}=1.65m \\ b_{cy}=b_{ty}+2s\tan\theta=0.2+2\times0.75\times\tan 35^{\circ}=1.25m \end{cases}$$

$$p=\frac{F}{A}=\frac{140}{2\times1.65\times1.25}=33.939\text{kN/m}^2$$

Vertical Soil Pressure: 17kN/m^3×0.75m=12.75kN/m^2

Coulomb Earth Pressure:

$$K_a=\frac{\cos^2(\phi-\alpha)}{\cos^2\alpha\cdot\cos(\alpha+\delta)\left[1+\sqrt{\frac{\sin(\phi+\delta)\sin(\phi-\beta)}{\cos(\alpha+\delta)\cos(\alpha-\beta)}}\right]^2}=\frac{\cos^2 25^{\circ}}{\cos^2 25^{\circ}\cdot\cos 37.5^{\circ}\left[1+\sqrt{\frac{\sin 37.5^{\circ}\sin 25^{\circ}}{\cos 37.5^{\circ}\cos 25^{\circ}}}\right]^2}=0.49$$

$$\sigma_a=\gamma HK_a=17\text{kN/}m^3\times12.35m\times0.49=102.8755\text{kN/}m^2$$

Surrounding Rock Pressure:

$$e=\gamma\left(H+\frac{1}{2}H_1\right)\tan^2\left(45-\frac{\phi_c}{2}\right)$$
$$=17\text{kN/m}^3\times\left(0.75+\frac{1}{2}\times11.6\right)\text{m}\times\tan^2(45^{\circ}-12.5^{\circ})=45.192\text{kN/m}^2$$

3 Burial Depth 1m

Vehicle Load:

$$\begin{cases} b_{cx} = b_{tx} + 2s\tan\theta = 0.6 + 2\times 1\times \tan 35^{\circ} = 2m \\ b_{cy} = b_{ty} + 2s\tan\theta = 0.2 + 2\times 1\times \tan 35^{\circ} = 1.6m \end{cases}$$

$$p = \frac{F}{A} = \frac{140}{2\times 2\times 1.6} = 21.875\text{kN/m}^2$$

Vertical Soil Pressure：$17\text{kN/m}^3\times 1\text{m}=17\text{kN/m}^2$

Coulomb Earth Pressure：

$$K_a = \frac{\cos^2(\phi - \alpha)}{\cos^2\alpha\cdot\ \cos(\alpha+\delta)\left[1+\sqrt{\frac{\sin(\phi+\delta)\sin(\phi-\beta)}{\cos(\alpha+\delta)\cos(\alpha-\beta)}}\right]^2}$$

$$= \frac{\cos^2 25^{\circ}}{\cos^2 25^{\circ}\cdot\ \cos 37.5^{\circ}\left[1+\sqrt{\frac{\sin 37.5^{\circ}\ \sin 25^{\circ}}{\cos 37.5^{\circ}\ \cos 25^{\circ}}}\right]^2} = 0.49$$

$$\sigma_a = \gamma H K_a = 17\text{kN}/m^3\times 12.6m\times 0.49 = 104.958\text{kN}/m^2$$

Surrounding Rock Pressure：

$$e = \gamma\left(H+\frac{1}{2}H_1\right)\tan^2\left(45-\frac{\phi_c}{2}\right)$$

$$= 17\text{kN/m}^3\times\left(1+\frac{1}{2}\times 11.6\right)\text{m}\times\tan^2\left(45^{\circ}-12.5^{\circ}\right) = 46.917\text{kN/m}^2$$

4 Burial Depth 1.25m

Vehicle Load：

$$\begin{cases} b_{cx} = b_{tx} + 2s\tan\theta = 0.6 + 2\times 1.25\times \tan 35^{\circ} = 2.35m \\ b_{cy} = b_{ty} + 2s\tan\theta = 0.2 + 2\times 1.25\times \tan 35^{\circ} = 1.95m \end{cases}$$

$$p = \frac{F}{A} = \frac{140}{2\times 2.35\times 1.95} = 15.276\text{kN/m}^2$$

Vertical Soil Pressure：$17\text{kN/m}^3\times 1.25\text{m}=21.25\text{kN/m}^2$

Coulomb Earth Pressure：

$$K_a = \frac{\cos^2(\phi - \alpha)}{\cos^2\alpha\cdot\ \cos(\alpha+\delta)\left[1+\sqrt{\frac{\sin(\phi+\delta)\sin(\phi-\beta)}{\cos(\alpha+\delta)\cos(\alpha-\beta)}}\right]^2}$$

$$= \frac{\cos^2 25^{\circ}}{\cos^2 25^{\circ}\cdot\ \cos 37.5^{\circ}\left[1+\sqrt{\frac{\sin 37.5^{\circ}\ \sin 25^{\circ}}{\cos 37.5^{\circ}\ \cos 25^{\circ}}}\right]^2} = 0.49$$

$$\sigma_a = \gamma H K_a = 17\text{kN}/m^3\times 12.85m\times 0.49 = 107.0405\text{kN}/m^2$$

Surrounding Rock Pressure：

$$e = \gamma\left(H+\frac{1}{2}H_1\right)\tan^2\left(45-\frac{\phi_c}{2}\right)$$

$$= 17\text{kN/m}^3\times\left(1.25+\frac{1}{2}\times 11.6\right)\text{m}\times\tan^2\left(45^{\circ}-12.5^{\circ}\right) = 48.642\text{kN/m}^2$$

5 Burial Depth 1.5m

Vehicle Load：

$$\begin{cases} b_{cx} = b_{tx} + 2s\tan\theta = 0.6 + 2\times 1.5\times \tan 35^{\circ} = 2.7m \\ b_{cy} = b_{ty} + 2s\tan\theta = 0.2 + 2\times 1.5\times \tan 35^{\circ} = 2.3m \end{cases}$$

$$p = \frac{F}{A} = \frac{140}{2\times 2.7\times 2.3} = 11.27\text{kN/m}^2$$

Vertical Soil Pressure：$17\text{kN/m}^3\times 1.5\text{m}=25.5\text{kN/m}^2$

Coulomb Earth Pressure：

$$K_a = \frac{\cos^2(\phi - \alpha)}{\cos^2\alpha \cdot \cos(\alpha+\delta)\left[1+\sqrt{\frac{\sin(\phi+\delta)\sin(\phi-\beta)}{\cos(\alpha+\delta)\cos(\alpha-\beta)}}\right]^2} = \frac{\cos^2 25^\circ}{\cos^2 25^\circ \cdot \cos 37.5^\circ\left[1+\sqrt{\frac{\sin 37.5^\circ \sin 25^\circ}{\cos 37.5^\circ \cos 25^\circ}}\right]^2} = 0.49$$

$$\sigma_a = \gamma H K_a = 17\text{kN}/m^3 \times 13.1m \times 0.49 = 109.153\text{kN}/m^2$$

Surrounding Rock Pressure：

$$e = \gamma\left(H + \frac{1}{2}H_1\right)\tan^2\left(45 - \frac{\phi_c}{2}\right)$$

$$= 17\text{kN/m}^3 \times \left(1.5 + \frac{1}{2} \times 11.6\right)\text{m} \times \tan^2(45^\circ - 12.5^\circ) = 50.367\text{kN/m}^2$$

4 Experimental Results and Analysis

4.1 Mechanical Performance without Vehicle Load

This section evaluates the mechanical performance of the entire span under different burial depths without applying vehicle load. Mises stress generally decreases from the left end and then increases, forming a parabolic shape with a minimum near the mid-span. Plastic strain follows a similar curve. Vertical displacement increases then decreases, also forming a parabolic trend. Generally, both Mises stress and plastic strain increase with burial depth. However, at 0.5m, a sudden increase occurs at the mid-span and nodes due to the additional impact of vehicle loads, resulting in greater displacement. From the diagrams, structural performance differs significantly at mid-span and endpoints. Table 4.1 lists the stress, strain, and displacement data for these critical points. For example, at 1.5m burial depth, Mises stress at mid-span reaches 518,369 Pa and vertical displacement peaks at 0.0519 m, indicating poorer performance. At 0.5m, endpoint Mises stress is highest at 847,898 Pa, plastic strain is 0.000016, and vertical displacement is 0.0013 m, showing weakest behavior at this depth.

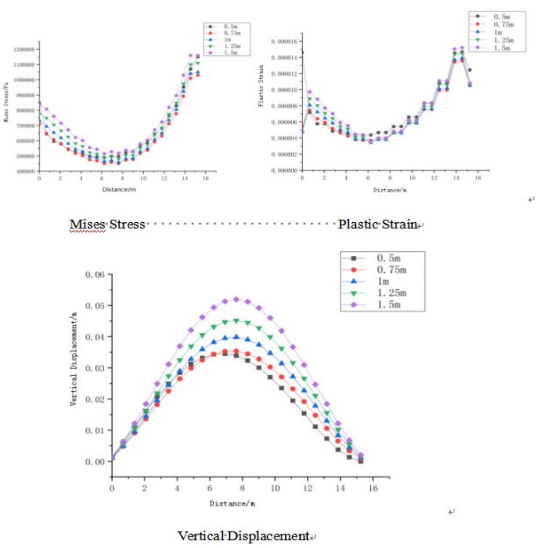

Figure4.1 Comparison diagram of mechanical properties of collapse without load

Table4.1 Mechanical properties of vulnerable point without load

Burial Depth	Mid-span			End Node		
	MisesStress/Pa	Plastic Strain	Vertical Displacement /m	MisesStress/Pa	Plastic Strain	Vertical Displacement /m
0.5m	498086	0.00000468	0.0345	847898	0.0000146	0.0013
0.75m	450056	0.00000400	0.0353	711808	0.0000055	0.0010
1m	458000	0.00000381	0.0398	732000	0.0000048	0.0011
1.25m	477730	0.00000383	0.0452	774611	0.0000047	0.0012
1.5m	518369	0.00000400	0.0519	835928	0.0000049	0.0014

4.2 Mechanical Performance with Vehicle Load

When vehicle load is applied, structural behavior across the span shows similar trends. Mises stress decreases then increases from left to right, with the lowest point at the mid-span. Plastic strain and vertical displacement again follow parabolic distributions. At shallow burial depths (0.5m and 0.75m), stress, strain, and displacement are significantly higher, especially near mid-span, indicating greater combined effects of vehicle and soil loads. At deeper burial depths, values are more stable and lower. From Table 4.2, the mid-span vertical displacement at 0.5m reaches 0.3144m, the highest among all cases. Endpoint values at 0.5m include Mises stress of 2, 278, 740 Pa, plastic strain of 0.0000243, and vertical displacement of 0.0151 m, again suggesting the weakest performance at shallowest depth.

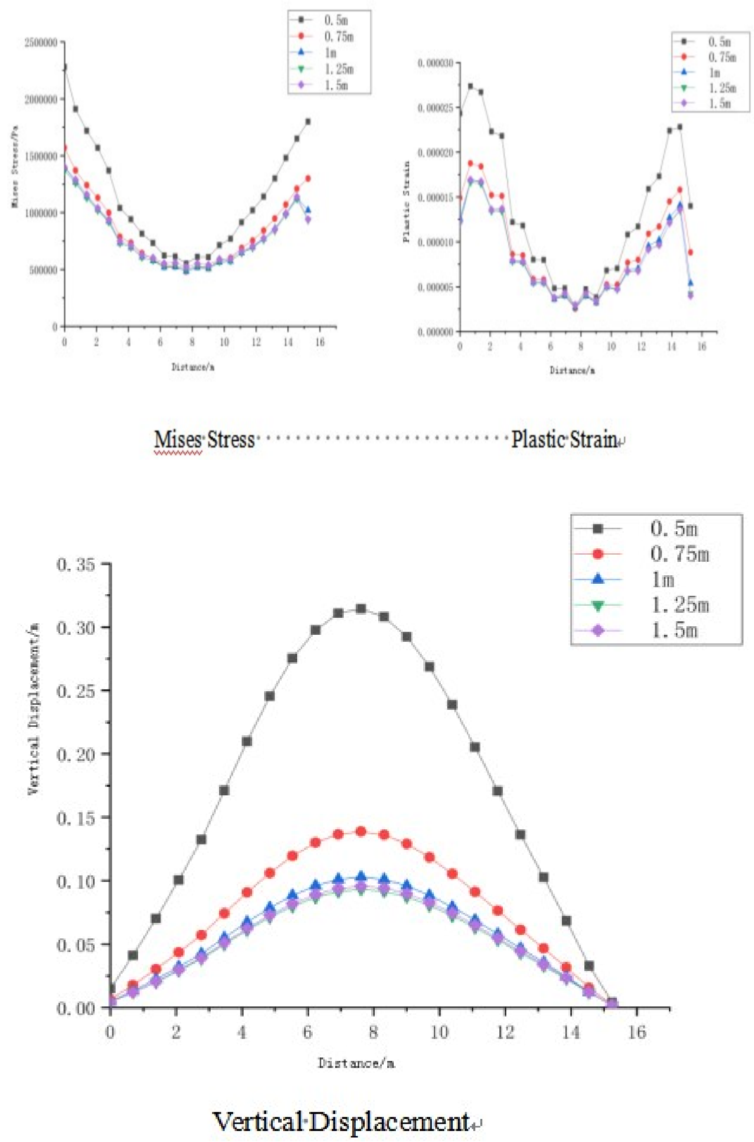

Figure 4.2 Comparison of mechanical properties of load collapse

Table 4.2 Mechanical properties of load collapse vulnerable point

Burial Depth	Mid-span			End Node		
	MisesStress/Pa	Plastic Strain	Vertical Displacement /m	MisesStress/Pa	Plastic Strain	Vertical Displacement /m
0.5m	551993	0.00000274	0.3144	2278740	0.0000243	0.0151
0.75m	482810	0.00000254	0.1389	1567890	0.0000149	0.0065
1m	484257	0.00000268	0.1030	1404260	0.0000126	0.0047
1.25m	500120	0.00000283	0.0933	1372790	0.0000121	0.0042
1.5m	522668	0.00000299	0.0958	1402080	0.0000123	0.0043

4.3 Mechanical Performance at Mid-Span Nodes

To better compare the mechanical performance of the structure at various burial depths, the mid-span node—where the greatest deformation occurs—is analyzed separately, as shown in Figure 4.3. The Mises stress and plastic strain at the mid-span node initially decrease with increasing burial depth and then gradually increase. The vertical displacement under vehicle loading also follows this trend. In contrast, under no vehicle load, the vertical displacement gradually increases. This indicates that the combined effect of vehicle load and soil overburden on the structure is not linear. Within the burial depth range of 0.75m to 1.25m, the Mises stress and plastic strain at the mid-span node remain relatively low, and vertical displacement is also minimal with only slight fluctuation .

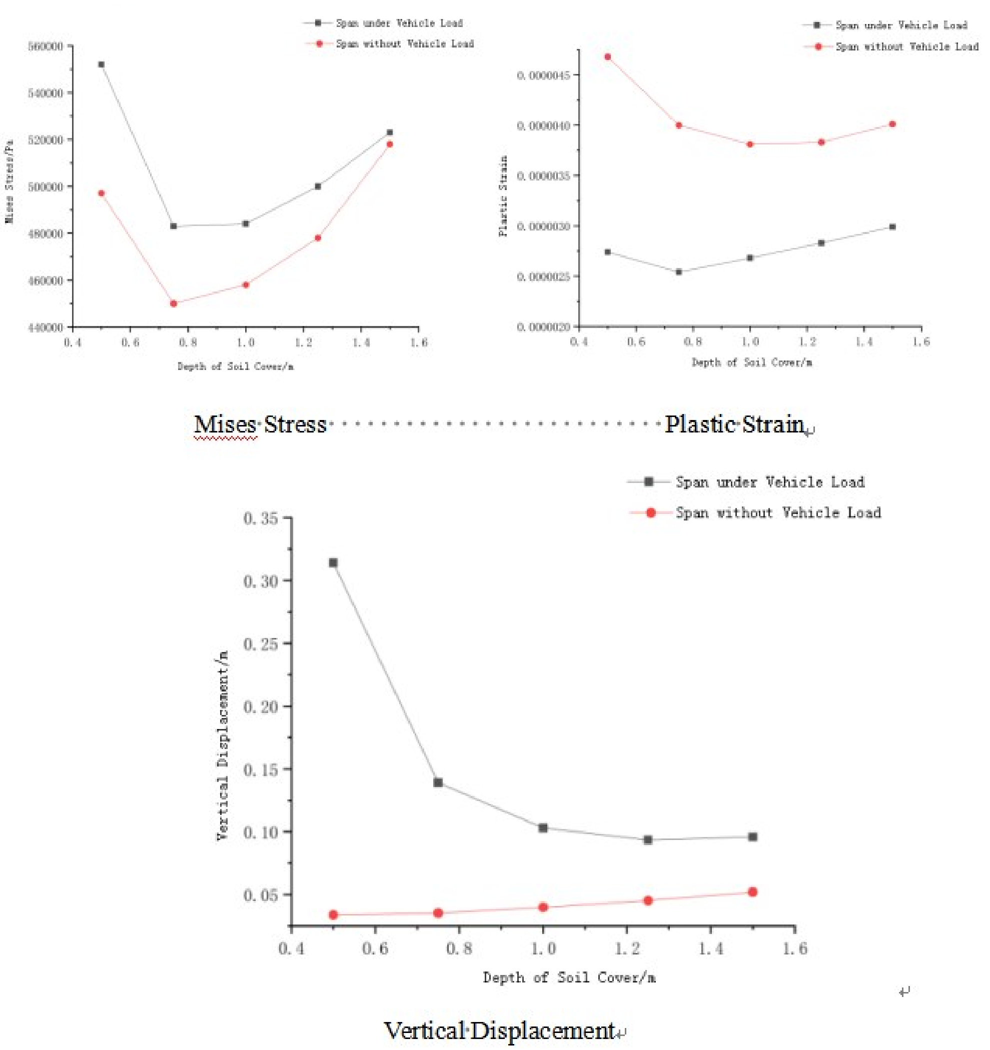

Figure 4.3 Mechanical performance of mid span joint

4.4 Analysis of Results

Based on finite element analysis using ABAQUS, the following conclusions were drawn: 1. The effect of burial depth on structural performance is not linear due to its interaction with vehicle loads. Both excessively shallow and deep burial depths negatively impact structural performance. 2. At depths of 1.25m–1.5m, mechanical performance without vehicle load deteriorates, as shown by elevated Mises stress, plastic strain, and vertical displacement. These conditions are less favorable structurally. 3. At 0.5m – 0.75m depths, the combined load from vehicles and overburden soil is significantly greater, causing more severe structural responses than at deeper depths.

5 Conclusion

Through mechanical analysis of structural performance at various burial depths, the shallow-buried underground complex primarily bears upper loads, including overburden soil and vehicle traffic. As burial depth increases, soil load increases, negatively affecting the structure, while vehicle load decreases, slightly reducing structural impact. Lateral stress from the soil has minimal effect and is negligible. The overall structural response does not decrease or increase uniformly with burial depth but follows a U-shaped trend. Both very shallow and very deep burial depths are structurally disadvantageous. Combining results across various burial depths, it is preliminarily concluded that the optimal burial depth range for structural performance lies between 0.75m and 1.25m.

About the Author

Youbin Bu, male, PhD student, Architectural Engineering, DONGSHIN UNIVERSITY, Naju-si, Jellanam-do,Korea, E-mail: 15069096986@163.com.

References

[1] Code for Design of Urban Underground Roads. CJJ221-2015.

[2] Code for Design of Highway Tunnels. JTG3370.1-2018.

[3] Zhang Zhichao. Finite Element Analysis of Single-Row Reinforced Shear Wall Components Based on ABAQUS [D]. Chongqing University, 2011.

[4] Lu Tiejian, Wang Penghao, Yang Shilong, Song Ning. Nonlinear Finite Element Analysis of Prefabricated Monolithic Concrete Shear Wall Joint [J]. Railway Science and Engineering, 2015, (02): 342–347.

[5] Wu Xiaolong. Study on Seismic Performance of Energy-Dissipating Link Type Prefabricated Shear Wall Structure [D]. Advisor: Li Hongnan. Dalian University of Technology, 2016.

[6] Zhao Weijian, Guo Wannian, Jin Qiao, Dui Xin. Development of Vertical Connection Forms of Prefabricated Shear Wall Structures [J]. Industrial Construction, 2014, (04): 115–121+59.

[7] Li Guoqiang, Huang Xiaokun, Li Ran, Li Gang, Liu Xuan, Li Zhelong. Experimental and Finite Element Analysis of Horizontal Joints of Prefabricated Shear Walls with Post-Cast Bottom Areas [J]. Building Science, 2014, (05): 45–51.

[8] Zhang Yannian, Ma Jiabao, Wang Yuanqing. Comparative Analysis of Connection Forms of Prefabricated Shear Walls [J]. Construction and Budget, 2014, (02): 30–34.

[9] Di Dongchao, Qiang Jian, Wang Jian. Study on Equivalent Uniform Live Load of Utility Corridors [J]. Special Structures, 2016, 33(06): 47–51.